JOURNAL OF VIROLOGY, May 2007, p. 4798–4807 Vol. 81, No. 9
0022-538X/07/$08.00+0 doi:10.1128/JVI.02471-06

Determination of the Ex Vivo Rates of Human Immunodeficiency Virus Type 1 Reverse Transcription by Using Novel Strand-Specific Amplification Analysis▽

David C. Thomas,[1,2] Yegor A. Voronin,[1]† Galina N. Nikolenko,[1] Jianbo Chen,[3] Wei-Shau Hu,[3] and Vinay K. Pathak[1]*

Viral Mutation Section, HIV Drug Resistance Program, National Cancer Institute at Frederick, Frederick, Maryland 21702,[1] Basic Research Program, SAIC-Frederick, Inc., NCI-Frederick, Frederick, Maryland 21702,[2] and Viral Recombination Section, HIV Drug Resistance Program, National Cancer Institute at Frederick, Frederick, Maryland 21702[3]

Received 9 November 2006/Accepted 14 February 2007

Replication of human immunodeficiency virus type 1 (HIV-1), like all organisms, involves synthesis of a minus-strand and a plus-strand of nucleic acid. Currently available PCR methods cannot distinguish between the two strands of nucleic acids. To carry out detailed analysis of HIV-1 reverse transcription from infected cells, we have developed a novel strand-specific amplification (SSA) assay using single-stranded padlock probes that are specifically hybridized to a target strand, ligated, and quantified for sensitive analysis of the kinetics of HIV-1 reverse transcription in cells. Using SSA, we have determined for the first time the ex vivo rates of HIV-1 minus-strand DNA synthesis in 293T and human primary CD4$^+$ T cells (~68 to 70 nucleotides/min). We also determined the rates of minus-strand DNA transfer (~4 min), plus-strand DNA transfer (~26 min), and initiation of plus-strand DNA synthesis (~9 min) in 293T cells. Additionally, our results indicate that plus-strand DNA synthesis is initiated at multiple sites and that several reverse transcriptase inhibitors influence the kinetics of minus-strand DNA synthesis differently, providing insights into their mechanism of inhibition. The SSA technology provides a novel approach to analyzing DNA replication processes and should facilitate the development of new antiretroviral drugs that target specific steps in HIV-1 reverse transcription.

Retroviral reverse transcriptases (RTs) convert a single-stranded viral RNA genome into a double-stranded DNA (4). Among the crucial events in the process of reverse transcription is initiation of minus-strand DNA synthesis to generate minus-strand strong-stop DNA, selective degradation of genomic RNA by RNase H, minus-strand DNA transfer, initiation of plus-strand DNA synthesis, formation of plus-strand strong-stop DNA, plus-strand DNA transfer and additional minus- and plus-strand DNA synthesis to complete the formation of viral DNA.

Several questions regarding the complex nature of human immunodeficiency virus type 1 (HIV-1) reverse transcription in cells remain unanswered; these questions include the efficiency of DNA synthesis initiation and strand-transfer events, the rates of RNA- and DNA-dependent DNA synthesis, and preferential inhibition of minus- or plus-strand DNA synthesis by RT inhibitors. Studies using purified RT and template (5, 7, 9, 12, 18) as well as endogenous reverse transcription reactions using permeabilized virions (1, 19, 23) have provided insights into these questions. Additionally, recent application of real-time PCR technology (2, 24) has greatly facilitated the analysis of reverse transcription in cell-based assays; however, like all PCR methods, the real-time PCR technique cannot distinguish between the two DNA strands and a system for quantitative strand-specific analysis of reverse transcription during the course of viral infection has not been available.

We have now developed a novel strand-specific amplification (SSA) assay for site-specific amplification and quantification of each strand during HIV-1 reverse transcription and used it to measure the relative abundance of HIV-1 reverse transcription products generated at distinct steps over the time course of viral infection. These studies have allowed us to measure the kinetics of minus-strand DNA synthesis in 293T cells as well as human primary CD4$^+$ T cells, one of the target cells of HIV-1 infection. We have also measured the kinetics of plus-strand DNA synthesis and the efficiencies of minus- and plus-strand DNA initiation and transfer in 293T cells. Finally, we have used SSA to analyze the effects of RT inhibitors on minus- and plus-strand DNA synthesis, which provide insights into their mechanism of inhibition.

MATERIALS AND METHODS

Plasmids and mutagenesis. HIV-1-based retroviral vector pHDV-EGFP, which expresses HIV-1 Gag-Pol and the enhanced green fluorescent protein (EGFP) from the Nef open reading frame and does not expresses HIV-1 Env, was kindly provided by Derya Unutmaz (Vanderbilt University Medical Center, Nashville, TN) (22). pHCMV-G expresses vesicular stomatitis virus G envelope (VSV-G) (26). Site-directed mutagenesis of the central polypurine tract (cPPT) in pHDV-EGFP was performed using the QuikChange XL site-directed mutagenesis kit (Stratagene, Inc.). The wild-type cPPT sequence (5′-AAAAGAAAAGGGGGG-3′) was modified by introducing six silent mutations (5′-AAGCGCAAGGGCGGC-3′; the substitutions are underlined). A restriction fragment (SbfI-SalI) containing the cPPT was subcloned into the pHDV-EGFP plasmid to generate pHIV-GFP-cPPT$^-$ and sequenced to confirm the presence of the desired mutations and the absence of the undesired mutations.

* Corresponding author. Mailing address: Viral Mutation Section, HIV Drug Resistance Program, Center for Cancer Research, National Cancer Institute-Frederick, P.O. Box B, Room 334, Frederick, MD 21702. Phone: (301) 846-1710. Fax: (301) 846-6013. E-mail: vpathak@ncifcrf.gov.

† Present address: Department of Human Biology, Fred Hutchinson Cancer Research Center, Seattle, WA 98109.

▽ Published ahead of print on 21 February 2007.

Preparation of virus particles. For most experiments, virus was prepared from a 293T-based cell line HIV-GFP2, which contains an undetermined number of integrated proviruses derived from pHDV-EGFP. To generate virus, HIV-GFP2 cells were plated at 2×10^6 cells per 100-mm-diameter dish and pretreated for 2 days before transfection with 1 μM 3′-azido-3′-deoxythymidine (AZT) for 10 h to prevent possible reinfection of transfected cells with produced virus. Calcium phosphate transfection (CalPhos transfection kit; Clontech) was performed using 4 μg of VSV-G-expressing plasmid (26). After 7 h, DNA-containing transfection solution with 1 μM AZT was removed by washing cells once with AZT-free medium, and fresh medium was then added to the cells. The virus was collected 17 h later and concentrated 10-fold by ultracentrifugation at 20,000 × *g* for 1 h. After resuspension, the virus was treated with DNase I (30 units/ml, 10 mM final concentration of $MgCl_2$) for 1 h at room temperature, divided into 1-ml aliquots, and frozen at −80°C.

For some experiments, virus was produced following transient transfection of 293T cells with pHDV-EGFP or pHIV-GFP-cPPT$^-$ and VSV-G-expressing plasmid, using the MBS mammalian transfection kit (Stratagene). The treatment of virus produced from the transfected cells with DNase I (105 U/ml, 10 mM $MgCl_2$, 3 h at room temperature) resulted in very low background levels, indicating little contamination with transfected DNA.

Time course for analyzing reverse transcription products in 293T cells. To study the kinetics of HIV-1 reverse transcription, a time course of infection with HIV-1 HDV-EGFP virus was performed. For infection, 2×10^6 or 6×10^5 293T cells were plated per 100-mm- or 60-mm-diameter dish, respectively, the day before infection. A virus preparation concentrated 10-fold by centrifugation was diluted 20-fold in Dulbecco's modified Eagle's medium. Two or 0.66 ml of diluted virus solution was used to infect 293T target cells plated on a 100-mm- or 60-mm-diameter dish, respectively. After infection for 30 min, the virus was removed, cells were washed twice with phosphate-buffered saline to remove any residual virus, and fresh medium was added to the plate. At the end of each time point, cells were washed twice with phosphate-buffered saline, resuspended in 2 ml of phosphate-buffered saline, pelleted, and frozen until DNA isolation. In a typical time-course experiment, one plate of cells was collected at either 30-min or 1-h intervals for up to 6 h postinfection. Total cellular DNA was isolated using the QiaAmp DNA blood kit (QIAGEN) and resuspended in 250 to 400 μl of water. Real-time PCR or SSA analysis was performed four times for each primer-probe set using 4 μl of this extracted DNA.

To monitor the efficiency of infection, the percentage of GFP-expressing cells was measured 48 h postinfection using flow cytometry (FACscan and Cell-Quest Software; Bectin Dickinson). In most experiments, 10 to 30% of the infected cells expressed GFP (multiplicity of infection < 1).

To analyze the effects of RT inhibitors on reverse transcription, 293T cells were pretreated with the inhibitors for 24 h and maintained in the presence of the drugs during and after the infection. The following concentrations of inhibitors were used: efavirenz (EFV), 9 nM; 2′,3′-dideoxyinosine (ddI), 50 μM; 3′-deoxy-2′,3′-didehydrothymidine (d4T), 4 μM; AZT, 1 μM. For each inhibitor, infection efficiencies were reduced 97 to 99% relative to a minus-inhibitor control infection, as determined by flow cytometry 36 h after infection.

Time course for analyzing reverse transcription products in primary CD4$^+$ T cells. Activated CD4$^+$ T cells were purified from human peripheral blood mononuclear cells using the CD4 positive isolation kit (Dynal Biotech) according to the manufacturer's instructions. Cells were infected with HDV-EGFP virus by spinoculation as previously described; briefly, the cells were incubated for 2 h at 1,200 × *g* at 10°C, followed by incubation at 37°C for 1 h (16). The cells were then washed four times to remove residual virus and placed back at 37°C. The cell samples for each time point during a time course were collected and processed as described above for 293T cells.

Oligonucleotides. All padlock probes, primers, and dual-labeled probes were synthesized by Integrated DNA Technologies, Inc. Padlock probes containing a 5′ phosphate group were chemically synthesized by standard phosphoramidite chemistry and purified by polyacrylamide gel electrophoresis by the manufacturer. All of the probes used in this study were 83-mers containing the following common spacer region of 49 bases: 5′-TTGCGACTCGTCATGTCTGAACTC TAGTGATCTTAGTGTCAGGATAGCT-3′. The target arms were directed against various minus- and plus-strand sites in pHDV-EGFP.

Amplification of ligated probes was performed using RCA-23 (5′-ACTAGA GTTCAGACATGACGAGT-3′) as the forward primer and REV-21 (5′-GAT CTTAGTGTCAGGATAGCT-3′) as the reverse primer. These primers were chemically synthesized with a 5′ OH. Dual-labeled probes used for real-time quantitative PCR were end-labeled with 5′ 6-carboxyfluoescein (FAM) and 3′ 6-carboxytetramethylrhodamine (TAMRA).

SSA assay. During the first step of SSA, a padlock probe was hybridized to a denatured target DNA and circularized by treatment with thermostable *Taq* DNA ligase (New England Biolabs). The 10-μl reaction mix contained 1× *Taq* DNA ligase buffer, 10^9 molecules of padlock probe, 12 units of *Taq* DNA ligase, and 4 μl of total cellular DNA extracted from infected cells as described above. After an initial incubation at 95°C for 5 min to denature the target DNA, ligation was performed during 20 cycles of denaturing at 95°C for 1 min and probe annealing and ligation at 50°C for 4 min, followed by a final incubation at 50°C for 10 min. Negative control reaction mixtures were prepared as described above except that either target DNA or *Taq* DNA ligase was omitted. For each of the 12 padlock probes, the ligation reaction mixtures were performed using serial dilutions of linearized pHDV-EGFP DNA and 25 ng of uninfected 293T cell DNA to generate a standard curve to calculate the copy numbers of target DNA samples.

Detection of ligated padlock probe products was monitored by first subjecting dilutions of the ligation reaction mixture to a modified RCA method using two primers, followed by quantitative real-time PCR using dual-labeled probes. Ligation reaction mixtures were diluted to 100 μl with water, and 5-μl aliquots were added to a reaction mixture (25 μl, final volume) containing 20 mM Tris-HCl (pH 8.8), 10 mM KCl, 10 mM $(NH_4)_2SO_4$, 2 mM $MgSO_4$, 0.1% Triton X-100, 200 μM concentrations of deoxynucleoside triphosphates, 500 nM (each) RCA-23 (forward) and REV-21 (reverse) primers, 100 nM dual-labeled probe, 1 unit of Platinum *Taq* DNA polymerase (Invitrogen), and 2.4 units of *Bst* DNA polymerase (large fragment; New England Biolabs). An initial incubation was performed at 63°C for 8 min for the two-primer RCA reaction, followed by 2 min of incubation at 94°C, which effectively denatured *Bst* DNA polymerase while simultaneously activating Platinum *Taq* DNA polymerase. Samples were then subjected to 40 cycles of PCR (94°C for 15 s and 60 to 63°C for 1 min). Fluorescence data were collected during the extension step using an ABI PRISM 7700 Sequence Detection System. Copy numbers of target DNA were calculated using the ABI PRISM 7700 Sequence Detection System software based on standard curves generated with serial dilutions of pHDV-EGFP in the ligation reaction mixtures.

To normalize for the amount of input DNA added to an SSA reaction, samples were measured by conventional real-time PCR with a primer-probe set specific for the cellular porphobilinogen deaminase (PBGD) gene (GenBank accession number M95623) (27) as previously described (25). The forward primer was 5′-AGGGATTCACTCAGGCTCTTTCT-3′, the reverse primer was 5′-GCAT GTTCAAGCTCCTTGGTAA-3′, and the probe was 5′-FAM-TCCGGCAGAT TGGAGAGAAAAGCCTG-TAMRA-3′. Final copy numbers after PBGD normalization and subtraction of 0-h copy numbers are expressed as percentages of the 6-h copy number.

The kinetics of minus-strand DNA transfer and initiation of plus-strand DNA synthesis at the polypurine tract (PPT) were determined by using probes 1, 2, and 7, which detect reverse transcription products derived from the long terminal repeats (LTRs). During reverse transcription, the 3′ LTR is first synthesized soon after minus-strand DNA transfer and the 5′ LTR is synthesized after plus-strand DNA transfer. The kinetics of accumulation of LTR products over the 6-h time course represents synthesis of both LTRs; analysis of the kinetics of accumulation of LTR-specific probes suggested that most of the synthesis of the 3′ LTR is completed within the first 3 h after infection. Therefore, the kinetics of minus-strand DNA transfer and plus-strand DNA synthesis initiation at the PPT were analyzed over a time course of 3 h instead of 6 h. Finally, the copy numbers of the minus-strand DNA products detected by probe 4, which are complementary to the central flap on the plus-strand DNA, were similar to those detected with probe 1.

RESULTS

Strategy for SSA assay. SSA is based on the use of single-stranded padlock probes, which specifically hybridize to a target strand at their 5′ and 3′ ends (14) (Fig. 1A). After infection with HIV-1, total cellular DNA (including nascent HIV-1 DNA) is isolated, denatured, and hybridized to a strand-specific padlock probe. The probe termini are ligated to form a circularized probe that is amplified using cascade rolling-circle amplification (RCA) (11, 21). The products of this reaction are quantified by real-time PCR using dual-labeled TaqMan probes (6). Twelve padlock probes (Fig. 1B and 1C) were designed to allow measurements of the kinetics of minus-strand DNA transfer (probes 1 and 2), minus-strand DNA synthesis (probes 3, 4, 5, and 6), plus-strand DNA synthesis

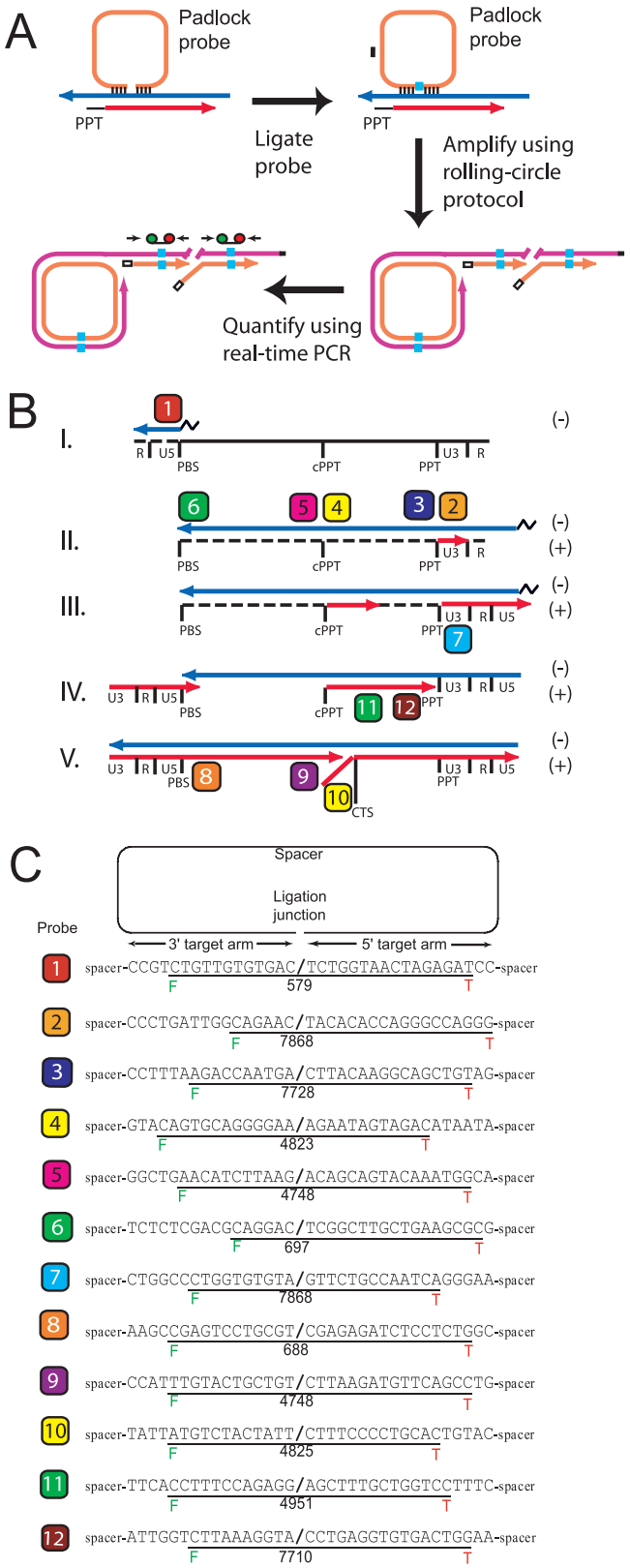

FIG. 1. SSA method for analysis of minus- and plus-strand DNA synthesis during HIV-1 reverse transcription. (A) Experimental strategy for SSA analysis. First (upper left), a single-stranded oligonucleotide (padlock probe) is hybridized at the 5′ and 3′ ends to one strand of a target nucleic acid (blue arrow). In this example, the padlock probe is shown as hybridizing to the minus-strand DNA adjacent to the PPT. Second, the 5′ and 3′ ends of the padlock probe are ligated to form a covalently closed circular DNA (blue square). A primer (black bar) is annealed to the circularized probe. Third, the circularized probe is amplified using a RCA protocol. A second primer (open bar) that anneals to the long single-stranded molecule generated through RCA is added to the reaction to exponentially amplify the probe sequences in a cascade reaction. Finally, the ligation junctions present in the RCA reaction are quantified using a real-time PCR amplification protocol (primers are shown as black arrows, and dual-labeled probes are labeled with green and red circles). (B) Padlock probes developed for SSA analysis of HIV-1 reverse transcription. A schematic outline of HIV-1 reverse transcription is presented. Solid black lines represent RNA, dashed black lines represent RNA degraded by the RNase H activity of RT, and blue and red lines represent minus- and plus-strand DNAs, respectively. Abbreviations: R, repeat region; U5, unique 5′ region; PBS, primer-binding site; cPPT, central polypurine tract; PPT, polypurine tract; U3, unique 3′ region; CTS, central termination sequence. For simplicity, only one of the two copackaged viral genomic RNAs is shown. The approximate locations of the ligation sites for padlock probes are indicated with numbers from 1 to 12 in color-coded boxes that are used throughout the figures. Probes 1 through 6 specifically detect minus-strand DNA products, whereas probes 7 through 12 specifically detect plus-strand DNA products. (C) As an example, the partial sequence of padlock probe 1, the ligation junction (slash), and the sequence of dual-labeled probe (underlined) are shown. The locations of the FAM (green F) and TAMRA (red T) fluorescent labels are indicated. A 49-base region that connects the target arms (spacer) is common to all probes. Probe 1 binds to a region that is located 56 nt 5′ of PBS.

initiation at the PPT (probes 2 and 7) and cPPT (probes 5 and 11), plus-strand DNA transfer (probes 6 and 8), plus-strand DNA synthesis (probes 8, 9, 11, and 12), and detection and quantification of the central flap (probe 10).

Determination of the sensitivity and accuracy of the SSA assay. To analyze the kinetics of HIV-1 reverse transcription, we generated VSV-G-pseudotyped HDV-EGFP virions by transfection with pHCMV-G of HIV-GFP2, a 293T-based cell line containing proviral copies of HDV-EGFP. The accuracy of quantitative real-time PCR assays is often compromised by contamination with the plasmid DNA used during transfection. To avoid this source of contamination, we used producer cells in which the viral DNA was stably integrated into the host cell chromosomal DNA. Another potential source of DNA contamination was reinfection of the viral producer cells, leading to reverse transcription and formation of viral DNA products after transfection with VSV-G-expressing plasmid. To suppress this possible source of DNA contamination, we maintained the producer cells in the presence of AZT to suppress reinfection of the producer cells.

The efficiency and background of SSA assay were determined for each of the 12 probes shown in Fig. 1B and 1C; representative results obtained from SSA analysis using probe 9 are shown in Table 1. High copy numbers of HIV-1-specific products (2×10^6 to 6×10^6) were detected 6 h after infection per SSA reaction, while the background copy numbers for 0 h control were less than 0.1% (313 copies), providing a strong signal-to-noise ratio. For some probes the background signals were higher, but never exceeded 1% (data not shown).

To estimate reproducibility of the SSA assay, the kinetics of accumulation of reverse transcription products detected with specific probes was determined in four independent experi-

TABLE 1. Time course for synthesis of HIV-1 plus-strand products detected by probe 9[a]

Time (h)	HIV-1 DNA copy no.[b]	PBGD copy no.[c]	PBGD normalization factor[d]	PBGD-adjusted HIV-1 copy no.[d]	PBGD-adjusted copy no. (0 h)[e]	% of 6-h HIV-1 copy no.[f]
0	313	313,385	1	313	0	0.00
0.5	1,145	211,683	0.6755	1,695	1,382	0.07
1	1,648	297,392	0.949	1,737	1,424	0.07
1.5	4,827	236,076	0.7533	6,408	6,095	0.30
2	38,443	304,567	0.9719	39,554	39,243	1.90
2.5	137,888	309,238	0.9868	139,732	139,424	6.75
3	331,356	204,398	0.6522	508,059	507,726	24.58
3.5	471,427	187,171	0.5973	789,263	789,007	38.19
4	1,017,892	262,514	0.8377	1,215,103	1,214,828	58.80
5	1,602,039	261,303	0.8338	1,921,371	1,921,039	92.99
6	2,199,462	333,590	1.0645	2,066,193	2,065,930	100.00

[a] Table represents one of four sets of measurements performed for probe 9 samples.
[b] Copy numbers were calculated as described in Materials and Methods based on standard curves generated with known amounts of pHDV-EGFP in the presence of 25 ng of uninfected 293T cell DNA.
[c] PBGD copy numbers were determined as described in Materials and Methods.
[d] The PBGD normalization factors (column 4) were calculated by dividing the PBGD copy number at each time point by the PBGD copy number at the 0-h time point. PBGD-adjusted HIV-1 copy numbers (column 5) were determined by dividing first the PBGD copy numbers (column 2) by the PBGD normalization factor (column 4).
[e] Final HIV-1 copy numbers (column 6) were calculated by subtracting the 0-h value (313) from the PBGD-adjusted copy numbers (column 5).
[f] Values were calculated as percentages of the final copy numbers divided by the 6-h copy number (2,065,930) and placed in column 2 of Table 2.

ments. Representative results obtained for probe 9 are shown in Table 2. For most experiments, the standard deviations were less than 20% of the average.

To control for efficiency of total DNA recovery, the copy numbers of the PBGD gene (27) were determined, which were within threefold of each other in most experiments, and used to normalize the levels of reverse transcription products. Analysis of reverse transcription products 6, 12, and 24 h postinfection indicated that the amount of viral DNA products peaked at 6 h (data not shown). Therefore, the PBGD-normalized copy numbers at 6 h postinfection were set to 100%, and the copy numbers obtained at earlier time points were expressed as a percentage of the 6-h copy numbers. To plot the kinetics of accumulation of reverse transcription products on a log scale, values less than 1% of the copy numbers obtained 6 h postinfection were set to 1%.

For analysis and comparison of data obtained from independent PCRs, the standard curves were generated by using the

TABLE 2. Summary of probe 9 copy numbers expressed as percentages of copy numbers at 6 h postinfection

Time (h)	% of 6-h copy no. for expt. no.:				Avg. % of 6-h copy no. (±SD)[b]
	1[a]	2	3	4	
0	0.00	0.00	0.00	0.00	1
0.5	0.07	0.02	0.24	−0.05	1
1	0.07	0.12	0.04	−0.03	1
1.5	0.30	0.17	0.27	0.04	1
2	1.90	2.55	2.78	2.44	2.42 ± 0.37
2.5	6.75	7.59	9.94	10.31	8.64 ± 1.76
3	24.58	19.73	12.60	19.94	19.19 ± 4.92
3.5	38.19	41.35	31.49	27.75	34.66 ± 6.17
4	58.80	68.97	53.01	71.16	62.93 ± 8.59
5	92.99	110.08	96.72	90.86	97.66 ± 8.63
6	100.00	100	100	100	100

[a] Values were taken from last column of Table 1.
[b] Values represent averages of results from four experiments (columns 2 to 5) and are expressed with standard deviations. Values less than 1 are set to 1 to generate a log-scale graph.

padlock probes to detect serially diluted samples containing known copy numbers of the target DNA and experimental samples; representative standard curves obtained for probes 3 and 11 are shown in Fig. 2A. The correlation coefficients were >0.99, indicating that the output signals were linear with respect to input DNA. All 12 strand-specific padlock probes reproducibly generated similar standard curves, indicating linear output signals. Note that the efficiency of amplification for all probes was different, as demonstrated for probes 3 and 11. For example, the observation that the signal for the known sample containing 10^7 copies was detected at cycle 14 by probe 3 and cycle 12 by probe 11 indicated that binding to the target sequence, efficiency of ligation, and/or efficiency of amplification with probe 3 is less efficient than with probe 11. Nevertheless, because the copy numbers in target DNAs were estimated from the standard curves, the efficiency of amplification does not influence the quantitation of target DNA copies.

The viral DNA copy numbers obtained using SSA were compared to the copy numbers obtained using an early RT primer probe set (R-U5) and standard quantitative real-time PCR (Table 3). The results showed that the copy numbers obtained using SSA were similar to those obtained using quantitative real-time PCR, except for the 0-h time point, because the background copy numbers using SSA were generally between 100 to 1,000 copies; thus, the SSA method does not have the sensitivity to accurately detect copy numbers below 1,000, but in samples containing higher copy numbers, the values obtained with SSA are comparable to those obtained with standard quantitative real-time PCR.

Rate of minus-strand DNA synthesis in 293T and primary human CD4$^+$ T cells. To determine the rate of minus-strand DNA synthesis, we performed SSA analysis with probes 3 and 6; representative experiments are shown in Fig. 2B using293T cells (left panel) and activated human primary CD4$^+$ T cells (right panel). The accumulation of reverse transcription products detected with each probe was expressed as a percentage of the copy number of products that accumulated at the 6-h time

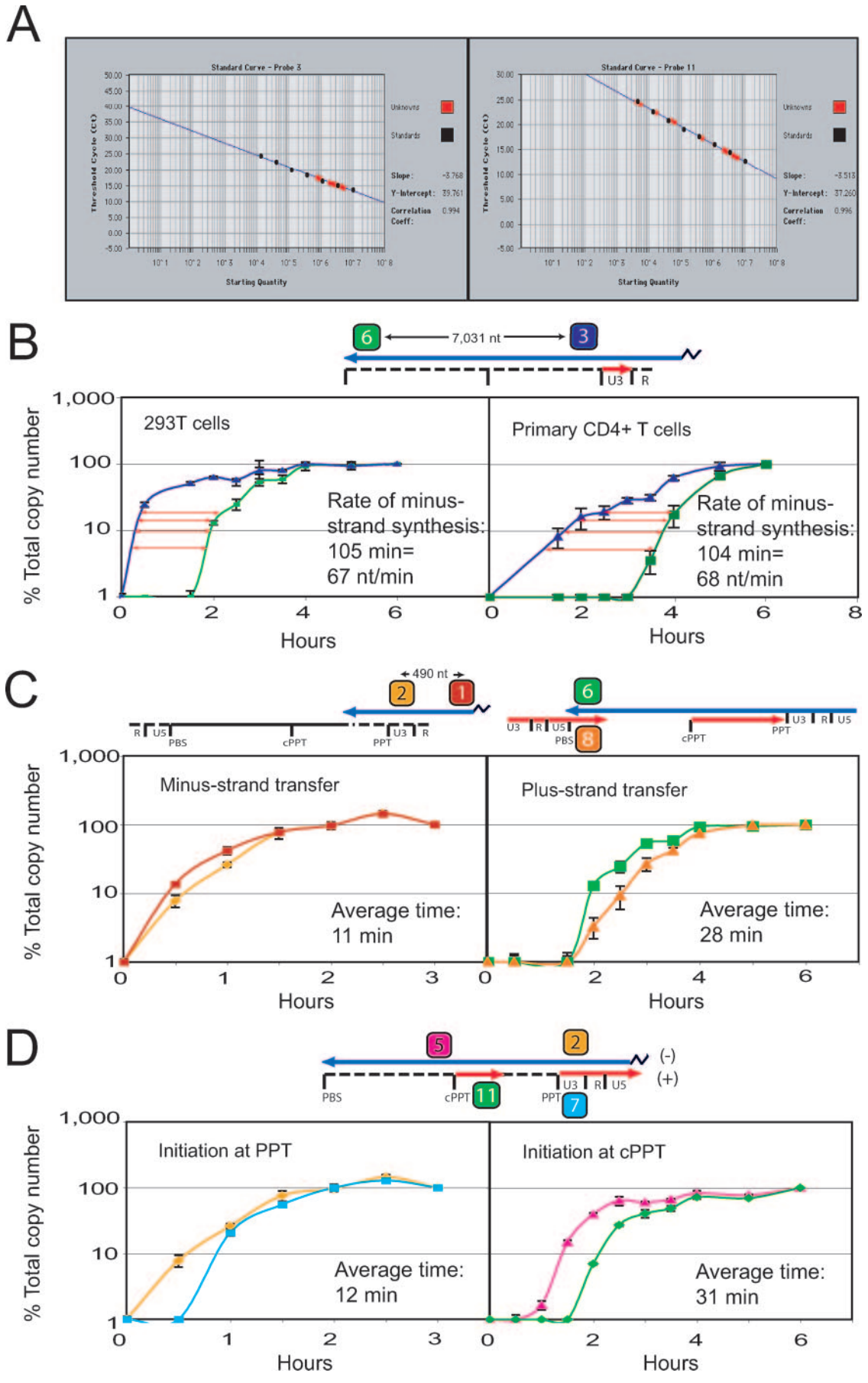
A
Standard Curve - Probe 3
Threshold Cycle (Ct)
Starting Quantity
Unknowns
Standards
Slope: -3.768
Y-Intercept: 39.761
Correlation Coeff: 0.994
Standard Curve - Probe 11
Slope: -3.513
Y-Intercept: 37.260
Correlation Coeff: 0.996
B
6
7,031 nt
3
U3
R
% Total copy number
293T cells
Rate of minus-strand synthesis: 105 min= 67 nt/min
Primary CD4+ T cells
Rate of minus-strand synthesis: 104 min= 68 nt/min
Hours
C
490 nt
2
1
6
R
U5
PBS
cPPT
PPT
U3
8
Minus-strand transfer
Average time: 11 min
Plus-strand transfer
Average time: 28 min
D
5
2
(-)
(+)
11
7
Initiation at PPT
Average time: 12 min
Initiation at cPPT
Average time: 31 min

TABLE 3. Comparison of real-time PCR and SSA analysis of time course for synthesis of early HIV-1 products[a]

Time (h)	PCR		SSA	
	Copy no.[b]	% of 6-h copy no.[c]	Copy no.	% of 6-h copy no.
0	465	0.03	1[d]	1
1	73,386	5.86	123,816	6.57
2	463,205	36.96	867,267	46.02
3	645,744	51.52	1,596,262	84.69
4	842,297	67.20	1,434,647	76.12
5	1,422,299	113.48	1,955,951	103.78
6	1,253,384	100	1,884,744	100

[a] Early HIV-1 products were measured with an R-U5 primer-probe set for real-time PCR analysis and padlock probe 1 (detecting minus-strand products) for SSA analysis.

[b] Copy numbers are averages of 2 to 4 sets of measurements performed using a standard curve and normalized to PBGD copy numbers (data not shown).

[c] The percentage of the 6-h copy number was calculated as the average copy number for each time point divided by the 6-h copy number.

[d] Note that the copy numbers for the 0-h time point are not comparable because the SSA method does not have the sensitivity to detect copy numbers below 1,000.

TABLE 4. Kinetics of HIV-1 minus-strand DNA synthesis[a]

Time course[b]	293T cells		Primary CD4$^+$ T cells	
	Time (min)	Rate[c] (nt/min)	Time (min)	Rate (nt/min)
1	105	67	104	68
2	109	65	96	73
3	95	74	104	68
4	157	45		
5	77	91		
Mean ± SD	109 ± 30	68 ± 17	101 ± 5	70 ± 3

[a] Minus-strand synthesis is measured as the progression of reverse transcription between probe sites 3 and 6 (see Fig. 1B), a distance of 7,031 nt.

[b] Time course 1 for each cell type is shown in Fig. 2A; the other time courses for each cell type are independent experiments performed under identical conditions.

[c] Rates for minus-strand DNA synthesis were calculated as described for Fig. 2A.

point. The distance between the curves representing the kinetics of accumulation of the products provided an estimate of the average time required for RT to copy the template between two probes. The average distance between the linear portions of the curves was determined by measuring the distance when the amounts of products accumulated were 5, 10, 20, and 30%.

The representative experiments displayed in Fig. 2B showed that the time required for minus-strand DNA synthesis to be extended from probe 3 to probe 6 (7,031 nt) was approximately 105 min for 293T cells and 104 min for human primary CD4$^+$ T cells, providing overall rates of DNA synthesis of 67 and 68 nucleotides (nt)/min, respectively. In 293T cells, the average rate of minus-strand DNA synthesis for five independent experiments, using probes 3 and 6 was 68 ± 17 nt/min, requiring an average of 109 ± 30 min (Table 4). In activated primary CD4$^+$ T cells, the average rate of minus-strand DNA synthesis for three independent experiments was 70 nt/min ± 3 min, requiring an average of 101 min ± 5 min. Thus, the rates of minus-strand DNA synthesis were very similar in 293T cells and activated primary CD4$^+$ T cells.

Kinetics of minus- and plus-strand DNA transfer. The kinetics of product accumulation detected by probes 1 and 2 and probes 6 and 8 were compared after infection of 293T cells to estimate the average time required for minus- and plus-strand DNA transfer, respectively. On average, ~11 min was required for extension of minus-strand DNA synthesis from probe 1 in U5 to probe 2 in U3 (Fig. 2C, left panel). At a rate of DNA synthesis of ~68 nt/min, approximately ~7 min was required for copying the 490 nt between probes 1 and 2. Since extension of minus-strand DNA synthesis from probe 1 to probe 2 re-

FIG. 2. Determination of the kinetics of minus-strand DNA synthesis, minus- and plus-strand DNA transfer, and initiation of plus-strand DNA synthesis using SSA analysis. (A) Standard curves for padlock probes 3 and 11 used in SSA analysis. Serial dilutions of pHDV-EGFP ranging from 4×10^3 to 1×10^7 in the presence of 25 ng of uninfected 293T cell DNA were subjected to SSA analysis to establish standard curves for padlock probes 3 (left panel) and 11 (right panel). Copy numbers of target DNA (red circles) were calculated using the ABI PRISM 7700 Sequence Detection System software based on the standard curve (black circles). (B) Rate of minus-strand DNA synthesis in 293T and human primary CD4$^+$ T cells. SSA analysis of HIV-1 reverse transcription using minus-strand specific padlock probes 3 and 6 is shown for time-course experiments performed with 293T cells (left panel) and human primary CD4$^+$ T cells (right panel). HDV-EGFP virus was used to infect 293T or human primary CD4$^+$ T cells and total cellular DNA was isolated from the infected cells at 30- or 60-min intervals for 6 h after infection. The accumulation of minus-strand DNA products detected with probes 3 and 6 was determined at each time point (see map above graph). The copy numbers of the products at 6 h after infection are set to 100%, and the products at earlier time points are presented as percentages of the copy numbers at the 6-h time point. To determine the rate at which reverse transcription proceeded from one probe to the next, the average distance between the curves (red arrows) generated for probes 3 and 6 was determined when the amounts of products accumulated were 5, 10, 20, and 30% of that at the 6-h time point. The time required for reverse transcription to proceed from probe 3 to probe 6 was approximately 105 and 104 min for 293T and human primary CD4$^+$ T cell time courses, respectively; since the distance between probes 3 and 6 is 7,031 nt, the rate of DNA synthesis was 67 and 68 nt/min for the 293T and human primary CD4$^+$ T cell time courses, respectively. (C) Determination of the rates of minus- and plus-strand DNA transfer using SSA analysis in 293T cells. The kinetics of minus-strand DNA transfer (left graph) was determined by the same technique used for minus-strand DNA synthesis except that the accumulation of products detected by probes 1 and 2 (see map above the left graph) was determined over a 3-h time course. The average time required for reverse transcription to proceed from probe 1 to probe 2 (~11 min) was determined as described above. The distance between probes 1 and 2 is 490 nt (see map above the left graph). The kinetics of plus-strand DNA transfer (right graph) was determined by measuring the accumulation of products detected with probes 6 and 8 (~28 min) over a 6-h time course. (D) Determination of the kinetics of plus-strand initiation at the PPT and cPPT in 293T cells. Initiation of plus-strand DNA synthesis at the PPT (left graph) was determined by the same technique used for minus-strand DNA synthesis except that the accumulation of products detected with probes 2 and 7 (see map above graph) were compared over a 3-h time course. Similarly, the kinetics of initiation of plus-strand DNA synthesis at the cPPT (right graph) was determined by analyzing the accumulation of products detected by probes 5 and 11 (see map above graph) over a 6-h time course. The average times indicated on each graph represent the delay in initiation of plus-strand DNA synthesis after minus-strand DNA synthesis has extended past the PPT (~12 min) and cPPT (~31 min).

quired ~11 min, a delay of ~4 min (~11 min to ~7 min) was associated with minus-strand DNA transfer.

Similarly, we determined the kinetics of plus-strand DNA transfer after infection of 293T cells by analyzing the accumulation of products detected by probes 6 and 8, which are located 3′ of the primer-binding site (PBS) and are specific for the minus and plus strand, respectively (Fig. 2C, right panel). On average, ~28 min was required for reverse transcription to proceed from probe 6 to probe 8. Since ~100 nt of DNA synthesis occurred during progression of reverse transcription from probe 6 to probe 8, requiring approximately 2 min for synthesis, a longer delay of ~26 min (~28 min to ~2 min) was associated with plus-strand DNA transfer.

Kinetics of plus-strand DNA synthesis initiation. The kinetics of initiation of plus-strand DNA synthesis at the PPT after infection of 293T cells were determined by analyzing the accumulation of products detected by probes 2 and 7, which are located 3′ of the PPT and are specific for the minus- and plus-strand, respectively (Fig. 2D, left panel). On average, ~12 min was needed for progression of reverse transcription from probe 2 to probe 7. Approximately 3 min (~68 nt/min) was required to incorporate ~200 nt during progression of reverse transcription from probe 2 to probe 7. Thus, a delay of ~9 min (~12 min to ~3 min) was associated with initiation of plus-strand DNA synthesis at the PPT.

Similarly, the kinetics of plus-strand DNA synthesis initiation at the cPPT was determined by analyzing the accumulation of products detected by probes 5 and 11 (Fig. 2D, right panel). An average of ~31 min was required for progression of reverse transcription from probe 5 to probe 11, whereas DNA synthesis (~200 nt) required ~3 min (~68 nt/min). Thus, a longer delay of ~28 min was associated with initiation of plus-strand DNA synthesis at the cPPT in comparison to the PPT.

Plus-strand DNA synthesis is initiated at multiple sites. To determine the rate of plus-strand DNA synthesis in 293T cells, we compared the kinetics of accumulation of products detected by plus-strand-specific probes 8, 9, 11, and 12 (Fig. 3A). The products detected by probes 11 and 12 accumulated with faster kinetics than products detected by probes 8 and 9, indicating that plus-strand DNA synthesis initiation at the cPPT and subsequent plus-strand DNA synthesis through probe 11 and 12 sites occurred ~30 min before minus-strand DNA synthesis reached the PBS to allow plus-strand DNA transfer and synthesis of products detected by probes 8 and 9. Probes 8 and 9 are 5′ of the cPPT and are separated by 4,060 nt, whereas probes 11 and 12 are 3′ of the central termination signal (CTS) and are separated by 2,759 nt. Despite the long distances separating these probes, the products detected by probes 8 and 9 accumulated with very similar kinetics, as did those of probes 11 and 12, implying either a very fast rate of plus-strand DNA synthesis or the presence of multiple sites for DNA synthesis initiation.

To determine whether additional sites of plus-strand DNA synthesis initiation contribute to the accumulation of plus-strand DNA products, we generated a cPPT$^-$ mutant by introducing four purine-to-pyrimidine substitutions within the cPPT sequence. The mutations in the cPPT did not significantly influence its ability to complete a single cycle of replication as determined by analysis of GFP expression in infected cells (data not shown). We observed that after infection with the cPPT$^-$ mutant, the products detected with probe 12 accumulated with faster kinetics than the products detected with probe 11 (Fig. 3B), indicating that plus-strand DNA synthesis was initiated at one or more sites between probes 11 and 12. Plus-strand DNA synthesis initiation at the cPPT was abrogated by the mutations in the cPPT because probe 11 products accumulated with kinetics similar to those for probe 8 and 9 rather than with the faster kinetics observed when the cPPT was wild type (Fig. 3A).

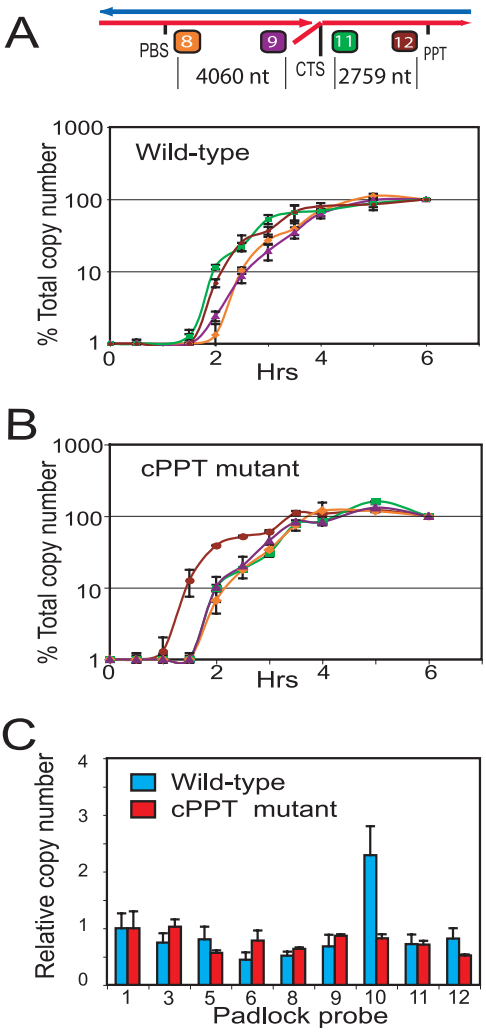

FIG. 3. SSA analysis of plus-strand DNA synthesis. (A) The kinetics of plus-strand DNA synthesis after infection with wild-type HDV-EGFP were determined by comparing the accumulation of products detected with probes 8, 9, 11, and 12 (see map above graph). Products detected with probes 11 and 12 accumulated with faster kinetics than products detected with probes 8 and 9. (B) The kinetics of plus-strand DNA synthesis after infection with the cPPT$^-$ mutant of HDV-EGFP were determined by comparing accumulation of products detected with probes 8, 9, 11, and 12 (see map above graph in panel A). Products detected with probe 12 accumulated with faster kinetics than those detected with probes 8, 9, and 11. (C) Efficiency of reverse transcription of wild-type HDV-EGFP (blue bars) or the cPPT$^-$ mutant of HDV-EGFP (red bars). The copy numbers of reverse transcription products detected with probe 1 at 6 h were set to a value of 1 (average value, 2×10^6 to 6×10^6 copies), and the copy numbers of products detected with various minus- and plus-strand probes (see Fig. 1B for location) are expressed relative to that of probe 1.

TABLE 5. Inhibition of HIV-1 replication with antiviral drugs

Drug	Drug concn	% Inhibition[a]
AZT	1 μM	98.44 ± 1.16
ddI	50 μM	97.46 ± 0.92
d4T	4 μM	98.97 ± 0.18
EFV	9 nM	99.37 ± 0.05

[a] The percentage of inhibition was calculated as 100% minus the percentage of cells in drug-treated samples that were positive for GFP expression, relative to the percentage of GFP-positive cells in the control infections in the absence of antiviral drugs. The percentage of GFP-positive cells was monitored by flow cytometry 36 h after infection. The results are shown as a means ± standard deviations from two independent experiments.

A comparison of the copy numbers of viral DNA products accumulated 6 h postinfection indicated similar copy numbers for most of the products (within twofold), indicating that after minus-strand DNA synthesis was initiated, the process of reverse transcription was efficient (Fig. 3C).

In contrast to most of the reverse transcription products, the product detected with probe 10 accumulated to a two- to three-fold-higher copy number level than the product detected by probe 1. Probe 10 was designed to detect the central flap (Fig. 1B), and two copies of probe 10 product were expected to be generated during reverse transcription; one copy would result from initiation at the cPPT and a second copy would result from plus-strand strong-stop DNA transfer followed by exten-

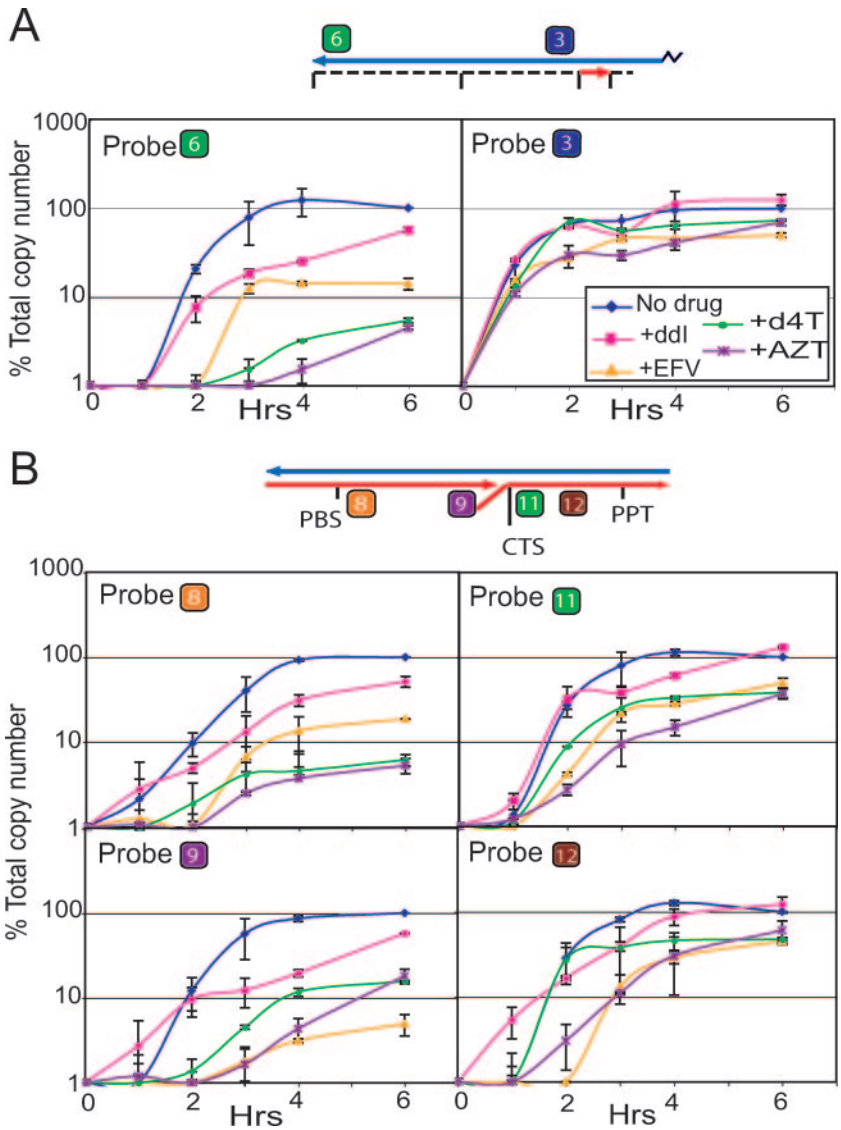

FIG. 4. SSA analysis of the effect of RT inhibitors on minus- and plus-strand DNA synthesis. (A) Effects of RT inhibitors on minus-strand DNA synthesis. The accumulation of products detected with probes 3 (right graph; see map above graph) and 6 (left graph) are compared over a 6-h time period in the absence of drugs (no drug) or presence of ddI, EFV, d4T, or AZT at concentrations that reduce viral titers by 95 to 99% (see Materials and Methods). (B) Effects of RT inhibitors on plus-strand DNA synthesis. The accumulation of products detected with probes 8 and 9 (left graphs) and 11 and 12 (right graphs; see map above graph) are compared over a 6-h time period in the absence (no drug) or presence of RT inhibitors. The results in panels A and B are expressed as percentages of the products accumulated at the 6-h time point in the absence of drugs. Symbol definitions are shown only for probe 3 but are the same for all probes.

sion of plus-strand DNA synthesis, leading to displacement of the synthesized DNA initiating at the cPPT. The detection of two to three copies of the products detected with probe 10 in comparison to the plus-strand DNA products detected with probes 9 and 11, which flank the central flap, indicated that the SSA analysis was able to quantitatively distinguish between one and two copies of reverse transcription products. As predicted, mutation of the cPPT (Fig. 3C) resulted in a lower copy number of products detected by probe 10 in comparison to the wild type, indicating that the central flap was no longer formed.

Effects of RT inhibitors on minus- and plus-strand DNA synthesis. To determine whether inhibitors of HIV-1 RT display differential effects during minus- and plus-strand DNA synthesis, we performed time course experiments in the presence of the nucleoside RT inhibitors ddI, d4T, and AZT and the nonnucleoside RT inhibitor EFV at concentrations that inhibited viral replication by 97 to 99% (Table 5 and Fig. 4). The inhibition of viral replication was monitored by performing fluorescence-activated cell sorter analysis to determine the percentage of infected cells that expressed GFP. The RT inhibitors had a minimal effect on the early minus-strand DNA products detected by probe 3 (Fig. 4A, right panel); in contrast, the late minus-strand DNA products detected by probe 6 accumulated to variable levels (Fig. 4A, left panel). In the presence of AZT and d4T, the probe 6 products accumulated to approximately 5% of the control levels; in comparison, the probe 6 products accumulated to approximately 15 and 55% of the control in the presence of EFV and ddI, respectively. Thus, minus-strand DNA synthesis was substantially inhibited by AZT and d4T, moderately inhibited by EFV, and minimally inhibited by ddI.

The accumulation of plus-strand DNA products detected by probes 8 and 9 (Fig. 4B, left panels) was inhibited to a similar extent compared to the probe 6 products (Fig. 4A, left panel), whereas the accumulation of products detected with probes 11 and 12 (Fig. 4B, right panels) was inhibited to a similar extent compared to the probe 3 products (Fig. 4A, right panel). This suggested a parallel between the accumulation of plus-strand DNA products and complementary minus-strand DNA products, which was most clearly evident for probes 6 and 8; for example, AZT and d4T inhibited the accumulation of probe 6 products to 5% of the control and a similar level of inhibition of probe 8 products was observed. Similarly, the accumulation of products detected by probes 11 and 12 was only modestly inhibited in the presence of RT inhibitors and was similar to the accumulation of probe 3 products (Fig. 4A); because a greater percentage of minus-strand DNA products were likely extended past the probe 11 and 12 binding sites, initiation at the cPPT or other internal sites may have resulted in higher levels of accumulation of probe 11 and 12 products than probe 8 and 9 products.

These results showed that AZT and d4T inhibited minus-strand DNA synthesis by 95% at drug concentrations that inhibited viral replication by 98% (approximately 20-fold). The observation that most of the inhibition of viral replication could be accounted for by the inhibition of minus-strand DNA synthesis suggests the intriguing possibility that AZT and d4T inhibited reverse transcription primarily during minus-strand DNA synthesis. However, inhibition of plus-strand DNA synthesis by AZT and d4T cannot be excluded. ddI and EFV inhibited minus-strand DNA synthesis by 45% and 85%, respectively, at drug concentrations that inhibited viral replication by >95%, implying that these RT inhibitors also impaired plus-strand DNA synthesis. Inhibition of plus-strand DNA synthesis could not be observed in these studies because it is initiated at multiple sites and reduction in plus-strand products is not cumulative, as is the case for minus-strand DNA synthesis.

DISCUSSION

The novel SSA assay described here should be applicable to a wide range of molecular studies in which quantification of specific strands of nucleic acids is desirable, including replication of other viruses (hepadnaviruses, adenoviruses, herpesviruses, etc.) and leading- and lagging-strand synthesis in organisms with double-stranded genomes. The SSA assay now further advances the quantitative PCR technology that has been applied to the measurements of HIV-1 viral load (3, 17), integrated DNA copies (2), and reverse transcription kinetics (2, 8, 24) by providing a tool for analyzing the strand-specific aspects of viral replication.

To our knowledge, these studies have provided the first measurements of several key steps during HIV-1 replication in cells, including the rate of minus-strand DNA synthesis (~68 to 70 nt/min). Previous measurements based on in vitro assays using either purified HIV-1 RTs (5, 7, 9, 12, 18) or endogenous reactions using components from permeabilized virions (1, 19, 23) varied greatly from 30 to 5,000 nt/min, presumably because the rates of DNA synthesis can be influenced by the assay conditions. The kinetics of HIV-1 replication probably also depend on intracellular conditions (15) and may exhibit cell-specific differences. Interestingly, the rates we obtained here for 293T cells and activated human primary $CD4^+$ T cells were very similar, suggesting that intracellular conditions such as deoxynucleoside triphosphate concentration are similar in these two cell types. However, we noted a delay in the kinetics for both probes 3 and 6 in human primary $CD4^+$ T cells, suggesting a possible delay in viral entry and early postentry steps, such as uncoating, delay in initiation of minus-strand DNA synthesis, or a delay in minus-strand DNA transfer (Fig. 2A). The SSA assay can also be used to determine the effects of specific mutations in viral proteins (RT, NC, Vif, Vpr, Nef, etc.) as well as *cis*-acting elements (PBS, PPT, cPPT, CTS, etc.) on the kinetics of various steps in HIV-1 replication.

The mechanism(s) that might contribute to the regional differences in the rate of minus-strand DNA synthesis are not known but could involve template RNA structures or greater availability of nucleocapsid protein later in replication, leading to more efficient denaturation of template structures, thereby increasing the rate of reverse transcription. The observation that plus-strand DNA transfer (~26 min) is much slower than minus-strand DNA transfer (~4 min) suggests that tRNA primer removal might be a slow and rate-limiting step. The observation that plus-strand initiation at the cPPT (~28 min) was much slower than at the PPT (~8 min) suggests that differences in sequences surrounding the two identical PPTs can influence the kinetics with which these plus-strand initiation sites are utilized.

Analysis of the $cPPT^-$ mutant of HIV-1 and the similar kinetics with which plus-strand products separated by long distances ac-

cumulated has provided strong evidence for multiple sites of plus-strand DNA synthesis initiation during replication in cells, as previously reported (10, 13). It is unclear at this time how many additional sites are used to initiate plus-strand DNA synthesis during HIV-1 replication, whether they represent specific sequences or RNA fragments that remain randomly associated with the minus-strand DNA, and how they avoid being displaced by DNA synthesis initiated at upstream sites.

Our observation that probe 10 products specifically detected two- to threefold-higher copy numbers of the central flap sequence, which has been implicated in the nuclear transport of HIV-1 preintegration complexes (20, 28), indicates that the SSA assay can provide a quantitative method for the detection of the central flap and could be used to analyze the efficiency of displacement synthesis in other regions of the HIV-1 genome.

In these studies, the inhibition of viral replication by AZT, d4T, and ddI was similar (97 to 99%), representing inhibition of minus- and plus-strand DNA synthesis. For AZT and d4T, most of the inhibition of viral replication could be attributed to the observed 95% inhibition of minus-strand DNA synthesis. However, ddI treatment resulted in 55% inhibition of minus-strand DNA synthesis, suggesting that ddI also inhibited viral replication during plus-strand DNA synthesis.

In summary, the SSA method should provide a widely applicable technology for strand-specific analysis of nucleic acids. The SSA assay described here can be used to address a variety of questions about the process of HIV-1 replication, elucidate the mechanism of action of antiretroviral agents, and facilitate development of novel antiviral agents that interfere with specific steps in HIV-1 reverse transcription.

ACKNOWLEDGMENTS

We thank Anne Arthur for expert editorial help. We also thank Rebekah Barr and Hongzhan Xu for technical assistance and Krista Delviks-Frankenberry and Eric Freed for critical readings of the manuscript.

This research was supported in part by the Intramural Research Program of the NIH, National Cancer Institute, Center for Cancer Research. This project has been funded in whole or in part with federal funds from the National Cancer Institute, National Institutes of Health, under contract N01-CO-12400.

The content of this publication does not necessarily reflect the views or policies of the Department of Health and Human Services, nor does mention of trade names, commercial products, or organizations imply endorsement by the U.S. Government.

REFERENCES

1. **Boone, L. R., and A. M. Skalka.** 1981. Viral DNA synthesized in vitro by avian retrovirus particles permeabilized with melittin. I. Kinetics of synthesis and size of minus- and plus-strand transcripts. J. Virol. **37:**109–116.
2. **Butler, S. L., M. S. Hansen, and F. D. Bushman.** 2001. A quantitative assay for HIV DNA integration in vivo. Nat. Med. **7:**631–634.
3. **Cesaire, R., A. Dehee, A. Lezin, N. Desire, O. Bourdonne, F. Dantin, O. Bera, D. Smadja, S. Abel, A. Cabie, G. Sobesky, and J. C. Nicolas.** 2001. Quantification of HTLV type I and HIV type I DNA load in coinfected patients: HIV type 1 infection does not alter HTLV type I proviral amount in the peripheral blood compartment. AIDS Res. Hum. Retrovir. **17:**799–805.
4. **Coffin, J. M., S. H. Hughes, and H. E. Varmus.** 1997. Retroviruses. Cold Spring Harbor Laboratory Press, Cold Spring Harbor, NY.
5. **Dube, D. K., and L. A. Loeb.** 1976. On the association of reverse transcriptase with polynucleotide templates during catalysis. Biochemistry **15:**3605–3611.
6. **Holland, P. M., R. D. Abramson, R. Watson, and D. H. Gelfand.** 1991. Detection of specific polymerase chain reaction product by utilizing the 5′—3′ exonuclease activity of Thermus aquaticus DNA polymerase. Proc. Natl. Acad. Sci. USA **88:**7276–7280.
7. **Huber, H. E., J. M. McCoy, J. S. Seehra, and C. C. Richardson.** 1989. Human immunodeficiency virus 1 reverse transcriptase. Template binding, processivity, strand displacement synthesis, and template switching. J. Biol. Chem. **264:**4669–4678.
8. **Karageorgos, L., P. Li, and C. J. Burrell.** 1995. Stepwise analysis of reverse transcription in a cell-to-cell human immunodeficiency virus infection model: kinetics and implications. J. Gen. Virol. **76**(Pt 7)**:**1675–1686.
9. **Kati, W. M., K. A. Johnson, L. F. Jerva, and K. S. Anderson.** 1992. Mechanism and fidelity of HIV reverse transcriptase. J. Biol. Chem. **267:**25988–25997.
10. **Klarmann, G. J., H. Yu, X. Chen, J. P. Dougherty, and B. D. Preston.** 1997. Discontinuous plus-strand DNA synthesis in human immunodeficiency virus type 1-infected cells and in a partially reconstituted cell-free system. J. Virol. **71:**9259–9269.
11. **Lizardi, P. M., X. Huang, Z. Zhu, P. Bray-Ward, D. C. Thomas, and D. C. Ward.** 1998. Mutation detection and single-molecule counting using isothermal rolling-circle amplification. Nat. Genet. **19:**225–232.
12. **Majumdar, C., J. Abbotts, S. Broder, and S. H. Wilson.** 1988. Studies on the mechanism of human immunodeficiency virus reverse transcriptase. Steady-state kinetics, processivity, and polynucleotide inhibition. J. Biol. Chem. **263:**15657–15665.
13. **Miller, M. D., B. Wang, and F. D. Bushman.** 1995. Human immunodeficiency virus type 1 preintegration complexes containing discontinuous plus strands are competent to integrate in vitro. J. Virol. **69:**3938–3944.
14. **Nilsson, M., H. Malmgren, M. Samiotaki, M. Kwiatkowski, B. P. Chowdhary, and U. Landegren.** 1994. Padlock probes: circularizing oligonucleotides for localized DNA detection. Science **265:**2085–2088.
15. **O'Brien, W. A., A. Namazi, H. Kalhor, S. H. Mao, J. A. Zack, and I. S. Chen.** 1994. Kinetics of human immunodeficiency virus type 1 reverse transcription in blood mononuclear phagocytes are slowed by limitations of nucleotide precursors. J. Virol. **68:**1258–1263.
16. **O'Doherty, U., W. J. Swiggard, and M. H. Malim.** 2000. Human immunodeficiency virus type 1 spinoculation enhances infection through virus binding. J. Virol. **74:**10074–10080.
17. **Palmer, S., A. P. Wiegand, F. Maldarelli, H. Bazmi, J. M. Mican, M. Polis, R. L. Dewar, A. Planta, S. Liu, J. A. Metcalf, J. W. Mellors, and J. M. Coffin.** 2003. New real-time reverse transcriptase-initiated PCR assay with single-copy sensitivity for human immunodeficiency virus type 1 RNA in plasma. J. Clin. Microbiol. **41:**4531–4536.
18. **Reardon, J. E.** 1993. Human immunodeficiency virus reverse transcriptase. A kinetic analysis of RNA-dependent and DNA-dependent DNA polymerization. J. Biol. Chem. **268:**8743–8751.
19. **Rothenberg, E., and D. Baltimore.** 1977. Increased length of DNA made by virions of murine leukemia virus at limiting magnesium ion concentration. J. Virol. **21:**168–178.
20. **Sirven, A., F. Pflumio, V. Zennou, M. Titeux, W. Vainchenker, L. Coulombel, A. Dubart-Kupperschmitt, and P. Charneau.** 2000. The human immunodeficiency virus type-1 central DNA flap is a crucial determinant for lentiviral vector nuclear import and gene transduction of human hematopoietic stem cells. Blood **96:**4103–4110.
21. **Thomas, D. C., G. A. Nardone, and S. K. Randall.** 1999. Amplification of padlock probes for DNA diagnostics by cascade rolling circle amplification or the polymerase chain reaction. Arch. Pathol. Lab. Med. **123:**1170–1176.
22. **Unutmaz, D., V. N. KewalRamani, S. Marmon, and D. R. Littman.** 1999. Cytokine signals are sufficient for HIV-1 infection of resting human T lymphocytes. J. Exp. Med. **189:**1735–1746.
23. **Varmus, H. E., S. Heasley, H. J. Kung, H. Oppermann, V. C. Smith, J. M. Bishop, and P. R. Shank.** 1978. Kinetics of synthesis, structure and purification of avian sarcoma virus-specific DNA made in the cytoplasm of acutely infected cells. J. Mol. Biol. **120:**55–82.
24. **Victoria, J. G., D. J. Lee, B. R. McDougall, and W. E. Robinson, Jr.** 2003. Replication kinetics for divergent type 1 human immunodeficiency viruses using quantitative SYBR green I real-time polymerase chain reaction. AIDS Res. Hum. Retrovir. **19:**865–874.
25. **Voronin, Y. A., and V. K. Pathak.** 2004. Frequent dual initiation in human immunodeficiency virus-based vectors containing two primer-binding sites: a quantitative in vivo assay for function of initiation complexes. J. Virol. **78:**5402–5413.
26. **Yee, J. K., A. Miyanohara, P. LaPorte, K. Bouic, J. C. Burns, and T. Friedmann.** 1994. A general method for the generation of high-titer, pantropic retroviral vectors: highly efficient infection of primary hepatocytes. Proc. Natl. Acad. Sci. USA **91:**9564–9568.
27. **Yoo, H. W., C. A. Warner, C. H. Chen, and R. J. Desnick.** 1993. Hydroxymethylbilane synthase: complete genomic sequence and amplifiable polymorphisms in the human gene. Genomics **15:**21–29.
28. **Zennou, V., C. Petit, D. Guetard, U. Nerhbass, L. Montagnier, and P. Charneau.** 2000. HIV-1 genome nuclear import is mediated by a central DNA flap. Cell **101:**173–185.